Preparation and Characterization of WO_3 Thick Film Resistors using Screen Printing Technique

S.J. Patil[1,*], A.V. Patil[2], K.S. Thakare[3], A.B. Patil[1] and R.R. Ahire[4]

[1]Department of Physics, L.V.H. College, Panchavati, Nashik, India
[2]Department of Physics, ASC College, Manmad, Dist.-Nashik, India
[3]Department of Physics, M.P.H. Mahila Mahavidyalaya, Malegaon, Dist.-Nashik, India
[4]Department of Physics, S.G. Patil College, Sakri, Dist.-Dhule, India

ABSTRACT

Tungsten trioxide (WO_3) thick films prepared by standard screen printing technique and fired at different temperatures in air atmosphere. The compositional, morphological and structural properties of films were analyzed by Field Emission scanning electron microscopy (FESEM), Energy dispersive spectroscopy (EDS) and X-ray diffraction (XRD). The films were observed to be oxygen deficient, it indicates that the films are non- stoichiometry in nature. As deposited and fired films were analyzed using SEM to know its surface morphology. XRD showed the polycrystalline nature. The crystallite size changes from 28.2133 nm to 58.5176 nm for all strong orientation with increase in firing temperature. The role of firing temperature on electrical resistivity has been studied and showed decrease in resistance with increase in temperature.

KEYWORDS: Thick films, XRD, FESEM, Structural properties, Electrical properties.

INTRODUCTION

To produce compact, robust and relatively inexpensive hybrid circuit for many purposes, Screen printing technique was introduced in the later part of 1950's, after that thick film technique has attracted by the sensor field[1]. Thick films are suitable for gas sensors since the gas sensing properties are mostly related to the material surface and the gases are always adsorbed and react with the films surface[2]. Screen printing is simple and economical method used to produce thick films of various materials[3-10]. The semiconducting metal oxides such as TiO_2, SnO_2, ZnO, Fe_2O_3, WO_3 etc. such type of semiconducting metal oxides (SMO's) offer the potential for developing portable and inexpensive gas sensing devices, which have advantages of simplicity, high sensitivity and fast response. The sensor is a device senses input signal. The working principle of these semiconductor gas sensors is based on change in conductivity when exposed to the target gases[11]. WO_3 is a widely studied transition metal oxide and behaves as n-type semiconducting oxide due to non- stoichiometry. It has been widely studied for several applications in optical fields and used as gas sensor. Several deposition methods have been used to grow WO_3 films such as Spray pyrolysis, Vacuum evaporation, chemical vapor deposition, magnetron sputtering, pulsed laser deposition, sol -gel technique, screen printing technique[12]. Among the various metal oxides that can be used in gas sensors, only those materials based on tungsten trioxide/titanium oxide have been widely manufactured and utilized[13].

EXPERIMENTAL

WO_3 Thick film preparation:

Table 1: Preparation of WO_3 films

Substrate material	Glass
Active Material	WO_3 (AR Grade)
Deposition Technique	Screen Printing
Types of screen	40S-Mesh No.355
Material Calcined time	1 hour.
Calcined temperature	4500c
Active Material to Organic vehicles ratio	70:30
Organic vehicles (Binders)	BCA & EC
Settling time	15-20 minutes.
Drying under IR	45 minutes.
Firing Time	2 hours.
Peak firing temp. (FT)	$350^{O}C$, $450^{O}C$ & $550^{O}C$

From table 1, the glass substrates used for screen printing were cleaned initially by soap solution. Further, they were cleaned by using chronic acid to remove the finger prints and other impurities present on the substrates. Finally substrates were washed by distilled water and then clean with acetone. Analytical Reagent (AR) grade WO_3 powder was calcined at 673K for an hour in a muffle furnace. Then this powder was crushed and thoroughly mixed. Organic vehicles such as butyl carbitol acetate (BCA) and ethyl cellulose (EC) were added to this active material to achieve proper thixotropic properties of the paste. The ratio of inorganic to organic parts was maintained at 70:30 (the ratio of EC to BCA was 98:2 in 30 %). WO_3 thick films were prepared on glass substrates using a standard screen-printing technique. The screen of nylon (40S, mesh no.355) was selected for screen-printing. The required mask was developed on the screen using a standard photolithography process. The paste was printed on clean glass substrates with the help of a mask. The pattern was allowed to settle for 15 to 20 minutes in air. The films were dried under infrared radiation for 45 minutes and fired at temperatures of $350^{O}C$, $450^{O}C$ &$550^{O}C$ for 2 h (which includes the time required to achieve the peak FT and then constant firing for 30 minutes at the peak temperature) in a muffle furnace.

Structural, morphological and compositional characterizations: The structural properties of WO_3 films were investigated using X-ray diffraction analysis for diffraction angle 2θ = 20-800 [D-8, Advance Model, Bruker diffractometer, Berlin, Germany] with Cu-*Kα* radiation of wavelength λ=0.1542 nm with a 0.10/step (2θ) at the rate of 2 s /step. FESEM [X-Flash Detector S-4800 type-II, Hitachi high Technology Corporation, Japan] was employed to characterize the surface morphology. The composition of WO_3 thick film samples were analyzed by an energy dispersive X-ray spectrometer (EDAX) [X-Flash Detector 5030, Bruker AXS GMBH]. The information about the grain shape and sizes of WO_3 thick film materials is obtained by using FESEM. All WO_3 samples were coated with a very thin conducting gold layer (few 100 Å) using vacuum sputtering technique to avoid charging of the samples. The composition of WO_3 thick film samples were analyzed by EDAX.

The crystallite size was determined using Scherer's formula[14].

$$D = \frac{0.9\lambda}{\beta\cos\theta} \qquad (1)$$

Electrical characterization: I-V characteristics were plotted for WO_3 samples annealed at 400°C. The DC resistance of the film samples as a function of temperature[15] was measured in home-built static measurement system.

The electrical resistivity (ρ) of thick film resistor was determined by using the equation,

$$\rho = (R \times A) / l \qquad (2)$$

$$\rho = \frac{[R \times b \times t]}{l}$$

where R = Resistance of WO_3 thick film at constant temperature; t = thickness of the film sample; l = length of the thick film; b = breadth of the thick film

The sample resistance measurement was carried out in static gas system[16-22] explained in the D.C. resistance measurement above. The static system consists of almost air tight glass bell-jar (chamber) in which heater, thermocouple and the sample mounted with electrodes for external electrical connections. The gas admittance valves are provided for injecting the target gas into the chamber of known volume. Sample resistance was measured in air ambiance and then in the presence of target gases with different concentrations and at various operating temperatures.

RESULTS AND DISCUSSION

Structural Parameters and their Analysis

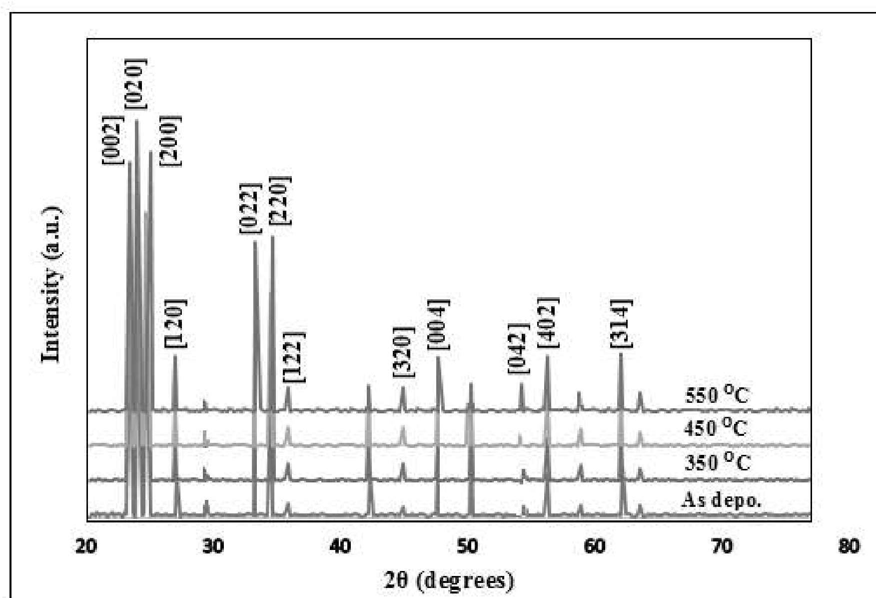

Fig. 1: XRD pattern of WO_3 films fired at (a) As deposited, (b) 350^OC, (c) 450^OC and (d) 550^OC.

Table 2. Variation of structural parameters for strong oriented peaks at different firing temperatures.

Firing Temp. ^OC	Plane (hkl)	d-values (A^O)	FWHM (β)degrees	Crystallite Size 'D' (nm)
As deposited	002	3.8275	0.285	28.4458
	020	3.7495	0.260	31.2087
	200	3.6377	0.288	28.2133
	120	3.3287	0.286	28.5411
	022	2.7234	0.285	29.0500
	220	2.5939	0.256	32.4857
	004	1.9111	0.288	30.1294
	402	1.6343	0.286	31.4825
350^OC	002	3.7762	0.240	33.7989
	020	3.7263	0.222	36.5608
	200	3.5986	0.284	28.6254
	120	3.3922	0.200	40.7710
	022	2.7234	0.218	37.9783
	220	2.5845	0.238	34.9549
	004	1.9179	0.206	42.0936
	402	1.6237	0.245	36.8199
450^OC	002	3.7668	0.228	35.5817
	020	3.7018	0.192	42.2859
	200	3.6217	0.194	41.8925
	120	3.3410	0.205	39.8100
	022	2.6962	0.178	46.5536
	220	2.6145	0.184	45.1633

	004	1.9317	0.188	46.0606
	402	1.6375	0.190	47.3630
550°C	002	3.8416	0.166	48.8302
	020	3.7608	0.154	52.6831
	200	3.6542	0.166	48.9381
	120	3.3225	0.166	49.1784
	022	2.7144	0166	49.8894
	220	2.6000	0.154	53.9899
	004	1.9208	0.166	52.2215
	042	1.7023	0.154	57.8250
	402	1.6401	0.154	58.5176

By using a standard screen printing method the films were deposited on glass substrate and fired at 350, 450, and 550°C. XRD analysis of WO_3 thick film samples analysis had been undertaken to understand the structure evolution and phase transformation of WO_3 thick film samples fired at 350, 450, and 550°C.

XRD analysis of WO_3 thick film samples were carried out in the 20-80° range using CuKα radiation with a 0.1^{O} /step (2θ) at the rate of 2 s /step. XRD analysis had been undertaken to understand the structure evolution and phase transformation of WO_3 thick film samples fired at 350, 450, and 550°C.

The crystalline structures of the thick films were analyzed with X-ray diffractogram. The diffraction peaks of crystal planes (002), (020), (200), (120), (022), (220), (122), (320), (004), (402) & (314) correspond to 2θ values of 23.1^{O}, 23.6^{O}, 24.3^{O}, 26.8^{O}, 32.9^{O}, 34.5^{O}, 35.5, 44.6^{O}, 47.3^{O}, 56.1^{O} & 63.2^{O} respectively, were obtained for as-deposited and fired at 350°C, 450°C, & 550°C thick film samples. In addition to these peaks, crystal plane (042) correspond to 53.8^{O} was also seen for the film fired at 550°C. From the XRD data, the obtained planes were found well matched with the standard JCPDS data card no. 83-0949, that show the presence of triclinic phase of WO_3 compound. From this analysis, several peaks of triclinic phases confirmed that the films were polycrystalline nature. The most reflected and strongly oriented peaks (002), (020), (200), (022), (220) were observed at 23.1^{O}, 23.6^{O}, 24.3^{O}, 32.9^{O}, 34.5^{O} indicate the growth of crystallites for preferred orientations along these particular directions.

Crystallite size (D) analysis: The crystallite size of WO_3 films at different FT is as shown in fig. 2. Generally, in the field of chemical sensors, the structural stability, porosity and high surface-to-volume ratio are key properties for a sensing film. Importantly, here, with increase in the FT, surface area will decrease as the grain size increases, which may drastically affect the gas sensing properties. The crystallite size of thick films as deposited and fired at different temperatures were determined using Scherer's formula.

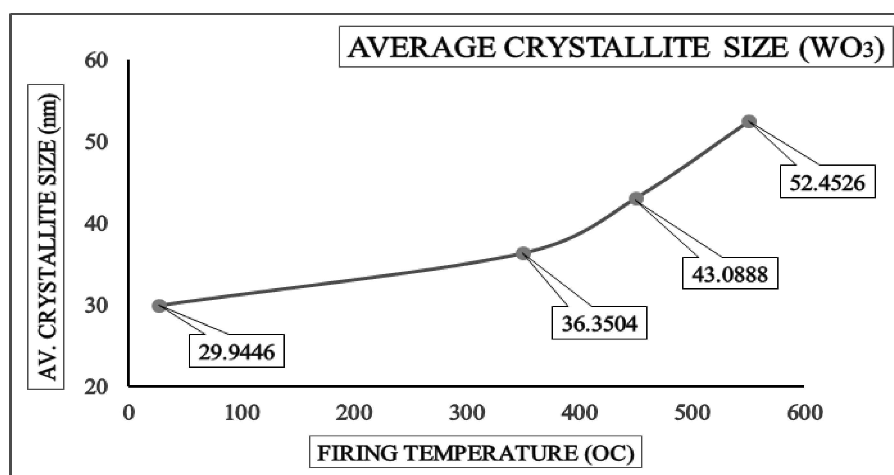

Fig. 2: Average crystallite size with different firing temperature.

Surface Morphology Analysis: The accelerated electrons carry significant amounts of kinetic energy & dissipated in different signals produced by interactions between the electron and film sample by Field Emission Scanning Electron Microscope (FESEM). These signals include secondary electrons, backscattered electrons, diffracted backscattered electrons, photons, visible light and heat. Images were produced by secondary electrons which can useful to studying the morphology of film samples, backscattered electrons are useful for illustrating rapid phase discrimination in multiphase samples. It was clearly seen that as-deposited samples revealed nano grains embedded into an amorphous matrix.

Fig.3 (a), (b), (c) and (d) represents the FESEM micrographs of WO_3 thick films. For comparison all images were recorded at same magnification. WO_3 thick films is made up of spherical grain structure. Increase in firing temperature FESEM images clearly showed that, the crystallite size increases & attributed to increase in the degree of crystallinity and grain size. Increase in grain & particle size increases the mobility of atoms at the surface of the film & thus decrease in the surface area[23].

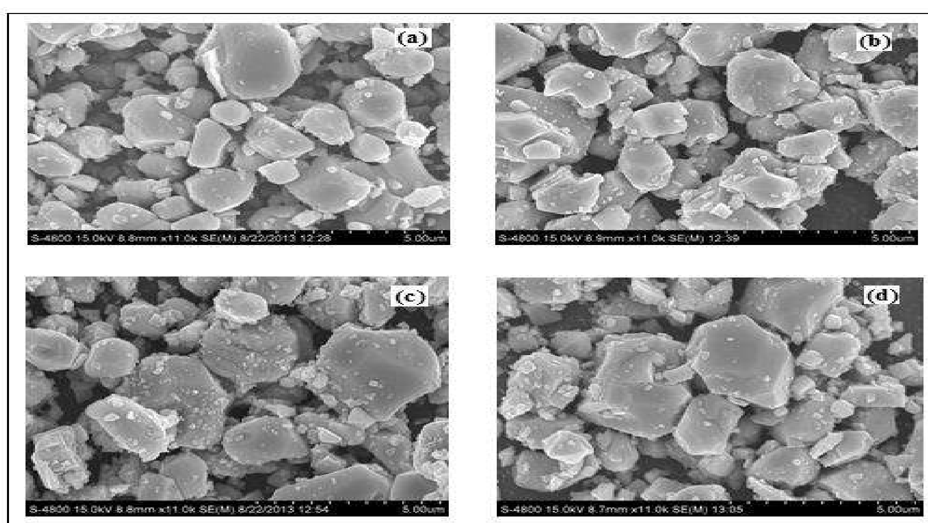

Fig. 3: FESEM of WO_3 thick films fired at (a) As deposited, (b) 350°C, (c) 450°C and (d) 550°C.

From FESEM images the particle size determination based on direct observations of particles and also receive the important information on the shape of particles. Surface morphology showed that the particle sizes are the function of the temperature. It has been observed that increase in the firing temperature leads to increase in porosity, increase in crystallite size, and decrease in oxygen which help to enhance the gas sensing performance.

Microstructure and specific surface area are the most important factors that influence the sensor characteristics. WO_3 thick films showing a spongy structure have a large fraction of atoms exist at surfaces and interfaces between the holes, the spongy surfaces of the films makes it highly suitable for gas sensing application.

Specific surface area can be determined from FESEM images. The specific surface area of WO_3 thick films was calculated for spherical particles using the equation[24].

$$Sw = \frac{6}{\rho . d} \quad (3)$$

where, d - Diameter of the particles and, ρ - Density of the particles.

Table 3: Specific surface area and particle size with the firing temperature.

Firing temperature	Specific Surface Area (m^2/g)	Particle size (nm)
As depo.	2.7032	310
350°C	2.3277	360
450°C	1.8417	455
550°C	1.6115	520

Energy Dispersive X-ray (EDAX) is a technique used for identifying the elemental composition of the film sample. The EDAX analysis system works as an integrated feature of scanning electron microscope[25, 26].

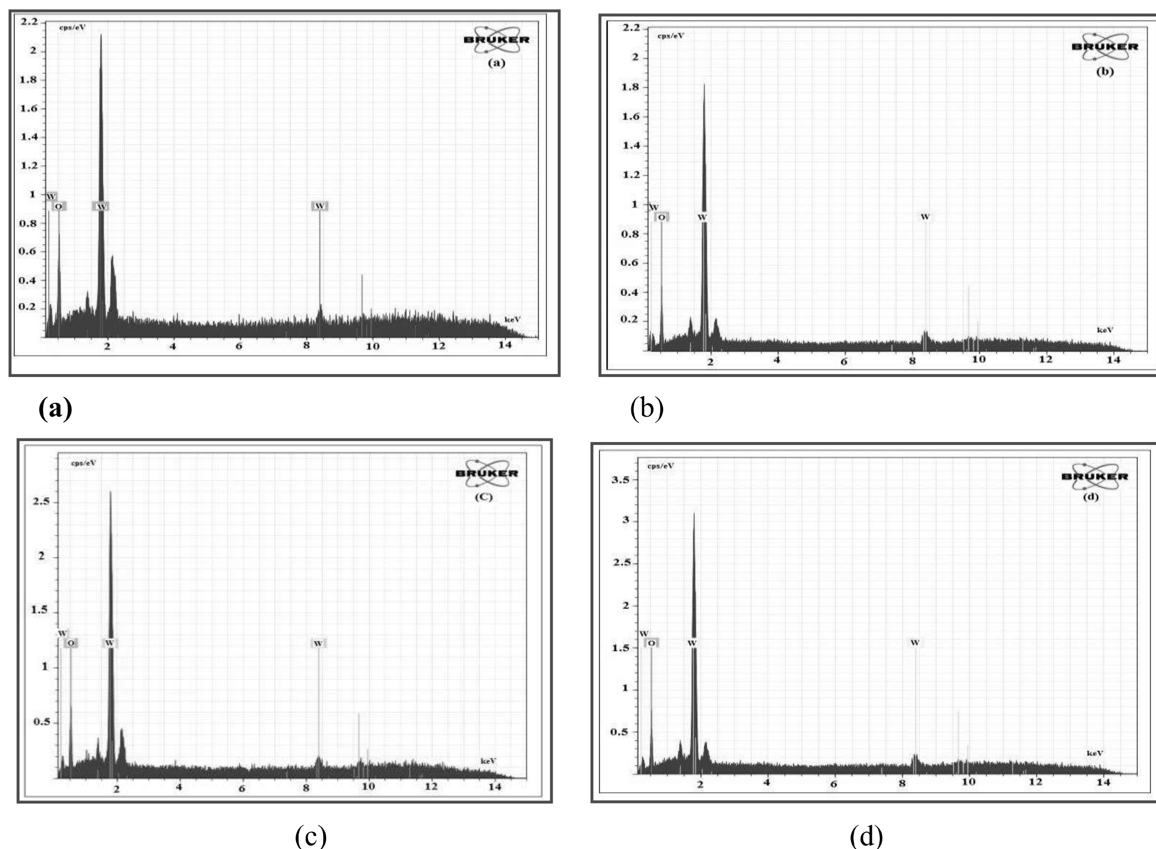

(a) (b)

(c) (d)

Fig. 4: EDAX spectrum of WO_3 thick films fired at (a) As deposited, (b) 350^OC, (c) 450^OC and (d) 550^OC

EDAX analysis reported the elemental composition of WO_3 thick films. Fig. 4 (a, b, c & d) spectrum reveals the presence of tungsten & oxygen elements without any impurity. Release of excess oxygen, mass percentage of W found to increase with increase in firing temperature[27]. Oxygen deficiency clearly indicates that the films are non-stoichiometry. The observed deficiency of oxygen show the conducting nature of WO_3[28, 29]. WO_3 thick films fired at 550^OC observed the high W/O ratio. Therefore the optimized firing temperature 550^OC selected for further studies of tungsten oxide thick films.

Table 4: Composition of WO_3 thick films.

Element (Mass %)	Firing Temperature			
	As deposited	**350^OC**	**450^OC**	**550^OC**
W	85.37	85.88	86.08	88.98
O	14.63	14.12	13.92	11.02

Electrical analysis: The resistance of WO_3 thick films decreased with increase in temperature shows semiconducting behavior. Resistivity increased with decrease in firing temperature.

I-V Characteristics: I-V characteristics of WO_3 thick films in air ambient shows the linearity which indicates the ohmic nature of the pressure contacts. Current versus voltage characteristics were measured for thick film samples in air ambient. Using constant voltage source ±30V, I-V characteristics were measured and presented in fig. 5 that shows the variation of current as a function of voltage.

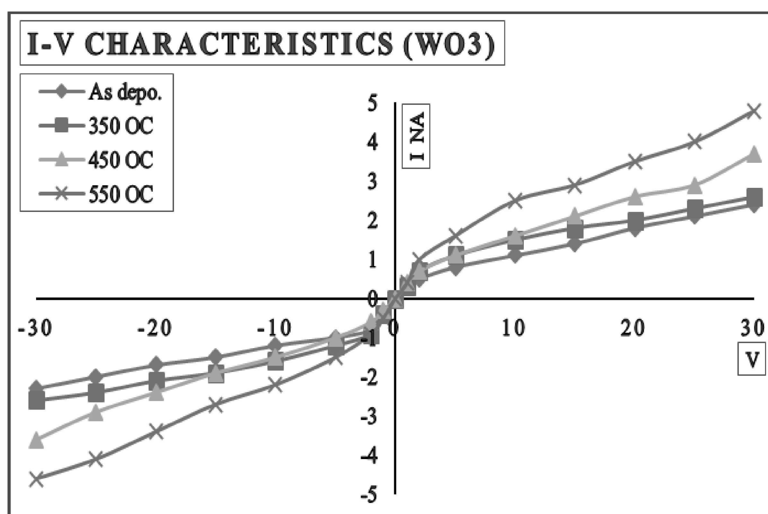

Fig. 5 I-V characteristics of WO_3 thick films fired at (a) as deposited, (b) $350^{O}C$, (c) $450^{O}C$ and (d) $550^{O}C$.

Resistivity (ρ): Electrical characterization of thick films observed that the resistivity decreases exponentially with increase in temperature could be attributed to negative temperature coefficient of resistance (NTC) and semiconducting nature of WO_3. Fig. 6 indicate that with variation in operating temperature, resistivity of thick films decreases with increase in firing temperature. Due to increase in firing temperature, increase in grain size results decreases in grain boundaries and associated impedance to the flow of charge carriers[30]. This behavior is favorable for gas sensing applications of thick films.

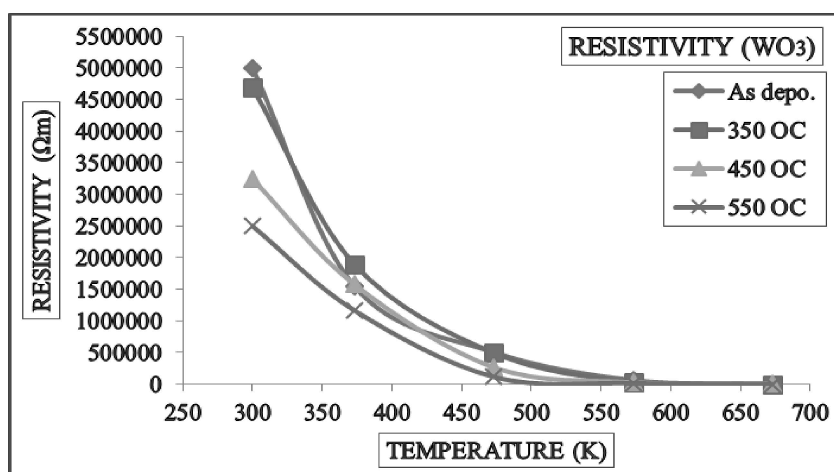

Fig. 6 Variation of resistivity (Ωm) with different firing temperatures.

Temperature dependent exponential variation of electrical resistivity depicted that the conduction mechanism is thermally activated. Onto the surface of SnO_2 oxygen adsorbs, & ionizes to O− or O_2− depending on the temperature by trapping electrons from the lattice[31]. Similar mechanism can be adopted in the case of WO_3. Increase in temperature, decrease in resistance of WO_3 thick films causes the electrons gain sufficient energy and cross over the barrier at grain boundaries, increasing drift mobility of the charge carriers or lattice vibrations where the atoms occasionally come closer enough for the transfer of charge carriers and conduction is induced by lattice vibrations[32]. The resistivity (ρ) of WO_3 thick films at constant temperature is calculated using the relation,

$$\rho = \frac{[R \times b \times t]}{l}$$

The resistivity of WO_3 thick films decreases with increase in firing temperature.

CONCLUSION

Small uneven shift in the peak positions has been observed due to increase in firing temperature of the thick films. It has detected that the peaks were randomly oriented since the obtained intensity of the peaks less than the standard intensity, by comparing the obtained intensity with the standard intensity. The increasing trend for the crystallite/grain size (nm) of thick films with an increase in the firing temperature has been observed.

The increasing trend found for the grain size of the film with an increase in the FT. The increase in the grain size may be due to the sintering of the smaller crystallites to form larger size crystallite after getting sufficient amount of thermal energy. With increase in the FT, surface area will decrease as the grain size increases

It was found that with increase in firing temperature, the smaller grains to come together to form a bigger grain as well as well-defined irregular shaped grains were seen without any amorphous matrix. Due to particle agglomeration, variations in particle size are also seen in FESEM images.

It has been observed that increase in the firing temperature leads to increase in porosity, increase in crystallite size,

From EDAX spectrum, the oxygen deficiency clearly indicates that the films are non-stoichiometry. The observed deficiency of oxygen show the conducting nature of WO_3.

Electrical characterization of thick films indicate that with variation in operating temperature, resistivity of thick films decreases with increase in firing temperature.

ACKNOWLEDGEMENT

The authors thank to Principal, L. V. H. College, Panchavati, Nashik, India, for providing laboratory facilities for present research work.

REFERENCES

1. N. Jaydev Dayan, S. R. Sainkar, R. N. Karekar and R. C. Aiyer, *Thin Solid Films*, **325**, 254 (1998).
2. K. Ram Kumar, *Thick Film Deposition and Processing Short Term Course on Thin and Thick Film Hybrid Microelectronics*, Bangalore **P 12.11** (1986).
3. B. Krishnan and V. N. Nampoori, *Bull. Mater. Sci*., **28**, 239 (2005).
4. X. Q. Liu, S. W. Tao and Y. S. Shen, *Sens. Actuators: B chemical* 40, 161(1997).
5. S. G. Ansari, P. Boroojerdian, S. K. Kulkurni, S. R. Sainkar, R. N. Karekar and R. C. Aiyer, *J .of Mater. Sci.* **7**, 267 (1996).
6. M. Prudenziati and B. Morten, *Sens. Actuators* **B10**, 65 (1986).
7. J. Kiran, R. B. Pant and S. T. Lakshmikumar, *Sens. Actuators* **B113**, 823 (2006).
8. A. T. Nimal, V. Kumar and A. K. Gupta, *Indian J. of Pure and Appl. Phys*. **42,** 275 (2004).
9. L. A. Patil L., P. A. Wani, S. R. Sainkar, A. Mitra, G. J. Pathak and D. P. Amalnerkar, *Mater. Chem. Phys*. **55**, 79 (1998).
10. C. A. Harper, *Handbook of Thick film hybrid Microelectronics*, McGraw Hill Book Co. New York, (1974).
11. A. Shrivastava and R. K. Jain, Mater. *Chem. Phys*., **105**, 385, (2007).
12. B. Joseph, K. G. Gopalchandran, P. K. Manoj, P. Koshy and V. K. Vaidyan, *Bull. Mater. Sci*. **22**, 921(1999).
13. K. Ihokura and J. Watson, The Stannic Oxide Gas Sensor: Principles and Applications, Boca Raton, FL: CRC Press, (1994).
14. B. D. Cullity, *Elements of X-ray Diffraction*, 2nd Edition, Addition Wesley, pp.102, (1970).
15. L. Gao, Q. Li, Z. Song and J. Wang, Preparation of nanoscale Titania thick film and its oxygen Sensitivity, *Sensors and Actuators **B**71*, pp. 179- 183, (2000).
16. S.K. Joshi, C. N. R. Rao, T. T. Suruto and S. Nagakura (Eds.) Narosa Publishing House, Ch-1 1-37, (1992).
17. Duk and Dong Lee, *Sensors and Actuators*, **B**, 231-235, (1990).
18. G. H. Jain and L. A. Patil, *Bulletin of Material Science*, **29 (4),** 403-411, (2006).
19. S. G. Ansari and S. G. Boroojerdianp, *J. of Mater. Sci-Mater. In Elect*. **7**, 267-270, (1996).
20. N. Jayadev Dayen, S. R. Sainkar, A. A. Belhekar, R. N. Karekar and R. C. Aiyer, *J. of Mater. Sci. Letters*, **16,** 1952-1954, (1997).
21. N. Jayadev Dayen, S. R. Sainkar, R. N. Karekar and R. C. Aiyer, *Measurement Science and Technology*, **9**, 360-365, (1998).
22. C. G. Dighavkar, Ph. D. Thesis, L. V. H. College, Panchavati, Nashik (MS) India, (2007).

23. I. S. Ahmed Frag, I. K. Battisha and M. M. EI_Rafaay, *Indian Journal of Pure Appl. Phys*. **43**, 446, (2005).
24. L. Gao, Li, Q., Song and Z. Wang, *Sens. Actuators*, **B71**, 179-183, (2000).
25. P. E. J. Flewit and R. K. Wild, Physical methods for material characterization , IOP Publishing Ltd. London, 501, (2003).
26. D. K. Schroder, Semiconductor material and device fabrication, John Wiley and Sons, 700, (1998)
27. E. San Andress, M. Toledano Luque, A. Del Prado, M. A. Navacerrada, G. Martill I. and Gonzalez Diaz, *Vac. Sci. Tech*., **A 23(6)** 1523-1530, (2005).
28. S. J. Pearton, D. P. Norton Ip K., Y.W. Heo, and T. Steiner, *Progress in Materials Science*, **50(3)**, 293-340, (2005).
29. 29. H. E. Brown, Zinc oxide: Properties and applications, International Lead Zinc Research Organization, Inc. New York, (1976).
30. S. Keshari, A. Kumar and D. Kabiraj, *Journal of nano Electron Phys*., **3 (1)**, 260-267, (2011).
31. N. Yamazoe, K. Ihokura and J. Watson (Eds.), The Stannic Oxide Gas Sensor: Principles and Applications, CRC Press, Boca Raton, 66, (1994).
32. K. Ramkumar, Characterization of Films, Short-Term Course on Thick and Thin Film Hybrid Microelectronics, Bangalore, (1986).